



Enzyme-modified Pt nanoelectrodes for glutamate detection

Journal:	<i>Faraday Discussions</i>
Manuscript ID	FD-ART-06-2024-000138
Article Type:	Paper
Date Submitted by the Author:	24-Jun-2024
Complete List of Authors:	Xu, Peibo; University of Illinois at Urbana-Champaign, Chemistry, Bioengineering Jetmore, Henry; University of Illinois at Urbana-Champaign, Chemistry Chen, Ran; University of Illinois at Urbana-Champaign, Chemistry; Southeast University, School of Chemistry and Chemical Engineering Shen, Mei; University of Illinois at Urbana-Champaign, Chemistry

ARTICLE

Enzyme-modified Pt nanoelectrodes for glutamate detection

Peibo Xu, (co-first author)^{†, a}, Henry David Jetmore (co-first author)^{†, a}, Ran Chen^{a, b}, and Mei Shen^{a, *}Received 00th January 20xx,
Accepted 00th January 20xx

DOI: 10.1039/x0xx00000x

We present here a glutamate oxidase (GluOx)-modified platinum (Pt) nanoelectrode with a planar geometry for glutamate detection. The Pt nanoelectrode was characterized using electrochemistry and scanning electron microscopy (SEM). The radius of the Pt nanoelectrode measured using SEM is ~210 nm. GluOx-modified Pt nanoelectrodes were generated by dip coating GluOx on the Pt nanoelectrode in a solution of 0.9% (wt%) bovine serum albumin (BSA), 0.126% (wt%) glutaraldehyde, and 100 U/mL GluOx. An increase in current was observed at +0.7 V vs. Ag/AgCl/1M KCl with adding increasing concentrations of glutamate. A two-sample t-test results showed that there is a significant difference for current at +0.7 V between the blank and the added lowest glutamate concentration, as well as between adjacent glutamate concentrations, confirming that the increase in current is related to the increased glutamate concentration. The experimental current-concentration curve of glutamate detection fitted well to the theoretical Michaelis-Menten curve. At the low concentration range (50 μ M to 200 μ M), a linear relationship between the current and glutamate concentration was observed. The Michaelis-Menten constants of I_{max} and K_m were calculated to be 1.093 pA and 0.227 mM, respectively. Biosensor efficiency (the ratio of glutamate sensitivity to H₂O₂ sensitivity) is calculated to be 57.9%. Enz_{act} (I_{max}/H_2O_2 sensitivity, an indicator of the amount of enzyme loaded on the electrode) of the GluOx-modified Pt nanoelectrode is 0.243 mM. We further compared the sensitivity of a GluOx-modified Pt nanoelectrode with a GluOx-modified carbon fiber microelectrode (7- μ m diameter and a sensing length of ~350 μ m). Glutamate detection on the GluOx-modified carbon fiber microelectrode fitted well to a Michaelis-Menten like response. Based on the fitting, the GluOx-modified carbon fiber microelectrode exhibited an I_{max} of 0.689 nA and a K_m of 301.2 μ M towards glutamate detection. The best linear range of glutamate detection on the GluOx-modified carbon fiber microelectrode is from 50 μ M to 150 μ M Glutamate. GluOx-modified carbon fiber microelectrode exhibited a higher potential requirement for glutamate detection comparing to the GluOx-modified Pt nanoelectrode.

Introduction

L-glutamate is the major excitatory transmitter at the insect and crustacean neuromuscular junction, as well as in the vertebrate central nervous system.¹⁻⁴ L-glutamate is essential for communication,⁵ learning and memory.⁶⁻⁸ Thus, the measurement of glutamate is important to understand the brain function. In addition, monitoring glutamate provides a means to better understand neurological diseases as abnormal regulation of glutamate is reported to be related to a number of neurological disorders such as Alzheimer's disease and depression.^{9, 10}

Currently, high performance liquid chromatography (HPLC) and chromatography-mass spectrometry (GCMS) are commonly used methods for glutamate detection.¹¹ But they include a separation method and take time. Electrochemical measurements allow for straightforward, label-free quantification of analytes with cost-effective devices and a short measurement time, making it a promising method for glutamate detection.

Glutamate is not electroactive therefore not able to be directly detected electrochemically. Enzyme modification is one common way to enable the electrochemical measurements for non-electroactive analytes.^{12, 13} Glutamate oxidase (GluOx) reacts with glutamate producing H₂O₂, which is electroactive and can be detected on the electrode surface directly. GluOx have been used to construct enzymatic glutamate electrodes by depositing an enzyme layer on top of the Pt electrode surface.¹⁴ However, most of these electrodes have micrometer to millimeter sizes. Pioneering work was carried out by Schulman group utilizing a GluOx-modified carbon nanoelectrode with cylindrical geometry for glutamate detection.¹⁵ Glutamate detection on GluOx-modified Pt nanoelectrodes with a planar geometry has not been reported.

It is unknown when the area of the electrode is decreased if the enzyme-modified nanoelectrodes have any analytical

^a Address: Department of Chemistry, University of Illinois at Urbana Champaign, Urbana, IL, 61801, USA

^b Current address: Current address: School of Chemistry and Chemical Engineering, Southeast University, Nanjing, 211189, China.

* Corresponding author, Email: mshen233@illinois.edu

[†] Equal Contribution, co-first author

Supplementary Information available: additional Figures including the following. Figure S1: Michaelis-Menten parameters calculation based on data in Figure 4, where $1/i$ was plotted as the y-axis and $1/c$ was plotted as the x-axis. Figure S2: Cyclic voltammograms of blank and glutamate on glutamate oxidase-modified Pt nanoelectrodes with three repeated runs overlapped. Figure S3: Box plot for current at +0.7 V vs. Ag/AgCl/1 M KCl from cyclic voltammograms of blank and glutamate solutions of different concentrations for the two-sample t-test. Figures S4 and S5: glutamate detection and related analysis on two additional GluOx-modified Pt nanoelectrodes. Figure S6: Michaelis-Menten parameters calculation for carbon fiber microelectrode. See DOI: 10.1039/x0xx00000x

sensitivity. This is because when the electrode area is smaller, a smaller number of enzymes will be loaded on the electrode surface. For the case of GluOx-modified nanoelectrode, less enzymes means less hydrogen peroxide will be produced. On the other hand, the hydrogen peroxide is produced in the immobilized enzyme layer of the enzyme-modified electrode. Thus, the diffusion of hydrogen peroxide maybe different from a hydrogen peroxide produced directly on the electrode surface without any surface layer. Consequently, the dilution of hydrogen peroxide produced on the immobilized enzyme layer may be less, which could help the sensitivity of the electrode. We propose to test this hypothesis by studying the enzyme-catalyzed reaction on a nanoelectrode with the smallest surface area, to the best of our knowledge, reported so far.

In this work, we present a novel enzymatic-Pt nanoelectrode with a radius of 210 nm and planar geometry for glutamate detection. This sensor was developed by the deposition of GluOx enzymatic layer on the surface of Pt nanoelectrode. This Pt nanoelectrode offers a significantly higher spatial resolution while maintaining a high sensitivity towards glutamate detection. The small size of our nanoelectrodes can minimize the damage to tissues when applied for in vivo study. More importantly, it has potential use in techniques such as scanning electrochemical microscopy (SECM).

Results and discussion

Fabrication and characterization of Pt nanoelectrodes. Pt nanoelectrodes were fabricated using a laser puller followed by focused ion beam milling. Detailed procedures were described under experimental section.

Scanning Electron Microscopy (SEM) was used to observe the resulted electrode after laser-pulling. The results are shown in Figure 1A, where the Pt appeared to protrude from the surrounding glass. In order to produce a disk geometry, focused ion beam (FIB) was used to mill this electrode. After FIB milling, the SEM result of the electrode was shown in Figure 1B, where the protruded Pt was no longer visible and a Pt nanoelectrode (a radius of ~ 210 nm) with planar geometry was observed.

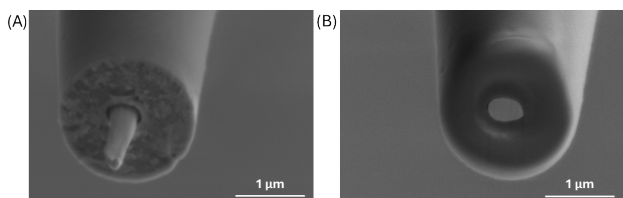


Figure 1. (A) SEM image of the Pt nanoelectrode after laser-pulling, Pt appeared to protrude from the surrounding glass. (B) SEM image of the Pt nanoelectrode after FIB milling, a planar geometry with a radius of about 210 nm was observed.

After SEM characterization, cyclic voltammetry was used to characterize the generated Pt nanoelectrodes. The cyclic voltammogram (CV) of the background electrolyte solution

was shown in dashed line in Figure 2A. After adding 0.5 mM Hexaamineruthenium (III) chloride (RuHex), the CV of reduction of RuHex was measured as solid line in Figure 2A. The background-subtracted CV of RuHex-reduction was shown in Figure 2B, where the CV exhibited a sigmoidal shape with a diffusion-limited current of 30.9 pA.

The electrochemical radius of the Pt nanoelectrode was calculated from the diffusion-limited current i_{ss} , which is expressed as the following equation,¹⁶

$$i_{ss} = 4xnFDCr \quad (1)$$

$$r = i_{ss}/4xnFD \quad (2)$$

where n is the number of electrons transferred, which is 1 in this case. F is Faraday constant, which is 96485 C/mol. D is the diffusion coefficient of RuHex in haemolymph-like (HL3) solution. A diffusion coefficient D of 5.48×10^{-6} cm²/s as reported in literature was used here.¹⁷ C is the concentration of RuHex, which is 0.5 mM. x is a function of RG, which is the ratio between the outer diameter (glass diameter) and inner diameter (Pt diameter). The glass radius measured from SEM image is around 928 nm. The Pt radius is ~ 210 nm based on the SEM image. The resulted RG is 4.39 and the calculated x is 1.043. The diffusion-limited steady state current measured at potential around -0.4 V vs Ag/AgCl/ 1 M KCl is 30.9 pA (Figure 2B). The electrochemical radius of the Pt nanoelectrode was calculated using equation (1) to be 280 nm. This electrochemical radius is slightly larger than SEM-observed geometric radius, suggesting the possibility of leaking (a gap existed between Pt and surrounding glass) cannot be ruled out. Regardless, the geometric size and electrochemical size is very close.

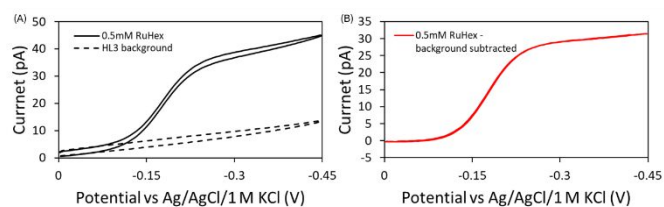


Figure 2. (A) Cyclic voltammogram (CV) of background (dashed line) and 0.5 mM RuHex (solid line). (B) Background-subtracted CV of 0.5 mM RuHex, which showed a sigmoidal shape.

Glutamate detection on glutamate oxidase (GluOx)-modified Pt nanoelectrode. We coated the Pt nanoelectrode described above with an enzyme, GluOx. Then we studied the response of the GluOx-modified Pt nanoelectrode towards glutamate detection. The mechanism of glutamate detection on the GluOx-modified electrode is shown in Figure 3. Glutamate reacts with water and oxygen, catalyzed by GluOx, producing H₂O₂. The generated H₂O₂ is detected on the Pt electrode via oxidation, generating a current. By measuring this current, glutamate is detected indirectly.

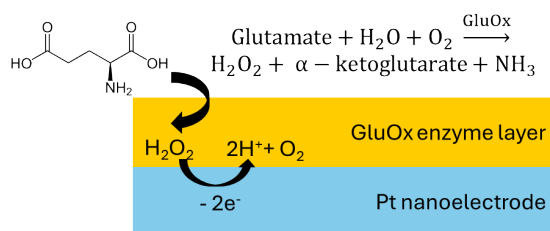


Figure 3. Mechanism of GluOx-modified Pt electrode for glutamate detection. Glutamate reacts in the enzyme layer catalyzed by GluOx to produce H_2O_2 . H_2O_2 is further detected on the Pt nanoelectrode surface via oxidation.

After placing the GluOx-modified Pt nanoelectrode into the HL3 background solution, the cyclic voltammogram (CV) of background solution was measured shown as the dashed black line in Figure 4A. After that, glutamate of different concentrations was added, and CVs were recorded following each addition. The forward curves of these CVs were plotted in Figure 4B. Figure 4C zoomed in the high potential range of Figure 4B, where we observed a clear increase in current with increased glutamate concentration. For instance, at 0.8 V, the current magnitude measured in background solution is 3.5 pA, and after adding 2 mM glutamate the current increased to 4.8 pA. Similarly, at 0.7 V, the current magnitude increased from 2.8 pA measured in background solution to 4.0 pA after adding 2 mM glutamate into the background solution. Similar observations were observed in two other GluOx-modified Pt nanoelectrodes discussed in a later section.

It is critical to make sure this increase in current is not due to the variability in CV measurements. To rule out this possibility, CVs were repeated for three times at each concentration of glutamate. The repeated CVs at each concentration overlapped very well (Figure S2), where it is hard to distinguish between different runs. This confirms that the current increase is likely due to the increased glutamate concentration. A two-sample t-test was performed to further confirm there is a difference in current after adding glutamate in comparison to blank solution. The two-sample t-test was performed between glutamate concentrations as shown in Figure S3. The current at +0.7 V vs. Ag/AgCl/1 M KCl (the potential of glutamate detection as described below) from three repeated CVs for background and all glutamate concentrations were used in the t-test. T-test results showed that there is a significant difference for current at +0.7 V between the blank and the added lowest glutamate concentrations, as well as between adjacent glutamate concentrations, confirming that the increase in current is related to the increased glutamate concentration.

We further compared the potential where an increase in current was observed with increasing glutamate concentrations to literature-reported glutamate detection potential. Several studies performed *i-t* chronoamperometry for glutamate sensing on GluOx-modified Pt microelectrodes.^{14, 18} The potential used was +0.6 V vs Ag/AgCl with

measurements often performed in 0.1 M phosphate-buffered saline (PBS) solution, which has a Cl^- concentration of ~ 0.014 M. Considering the concentration of Cl^- matters in the potential of the Ag/AgCl reference electrode, we converted the literature reference electrode potential to ours. We calculated the reference electrode potential with Nernst equation as shown in experimental section. +0.6 V vs Ag/AgCl in 0.1 M PBS is the same as +0.71 V vs Ag/AgCl/1 M KCl, which is the reference electrode in this study. +0.7 V is also the potential where we observed a clear increase in current in our CV. This is why we picked the potential of +0.7 V vs Ag/AgCl/1M KCl for constructing calibration curve.

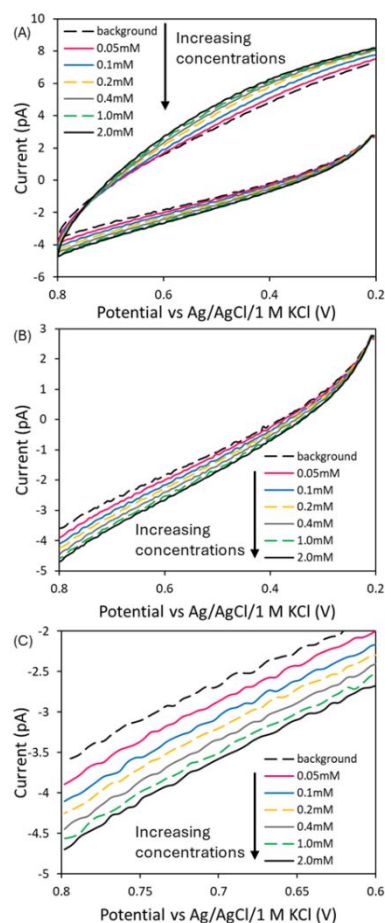


Figure 4. (A). Glutamate detection on the glutamate oxidase-modified Pt nanoelectrode (radius = 220 nm based on SEM shown in Figure 1B) using cyclic voltammetry (CV). (B). Forward linear sweep voltammogram from +0.2 V to +0.8 V vs. Ag/AgCl/1M KCl. (C). Zoom in on Figure B at high potentials where glutamate detection was reported in literature. Glutamate concentrations were shown in figure legends.

Figure 5A showed the overall calibration curve with glutamate concentration up to 2mM. The curve showed a Michaelis-Menten like response which was verified based on theoretical fitting as discussed later. Figure 5B showed the calibration curve at low concentration range (up to 200 μM), a linear relationship between the current and glutamate concentration was observed. The calculated sensitivity is 2.6059 pA/mM (slope of the linear regression line). Though this sensitivity

seems to be low, considering the nanometer size (radius of ~ 280.2 nm) of the electrode, the area-normalized sensitivity is $1.057 \times 10^{-5} \text{ nA } \mu\text{M}^{-1} \mu\text{m}^{-2}$.

Figure 5C showed the fitting of background-subtracted experimental data to the Michaelis-Menten curve, where a nice overlap between the experimental data (red dot) and the theoretical Michaelis-Menten curve was observed ($R^2 = 0.99$). The Michaelis-Menten constants of I_{max} and K_m were calculated to be 1.093 pA and 0.227 mM , respectively (the detailed calculation was shown in experimental section and SI). This K_m value is in the same order of magnitude with a slightly smaller number compared with other GluOx enzymatic glutamate microelectrode¹⁹⁻²² in the range of $0.22 \text{ mM} - 1.3 \text{ mM}$ while slight larger than another enzymatic glutamate nanoelectrode which presented a K_m of 0.06 mM .¹⁵

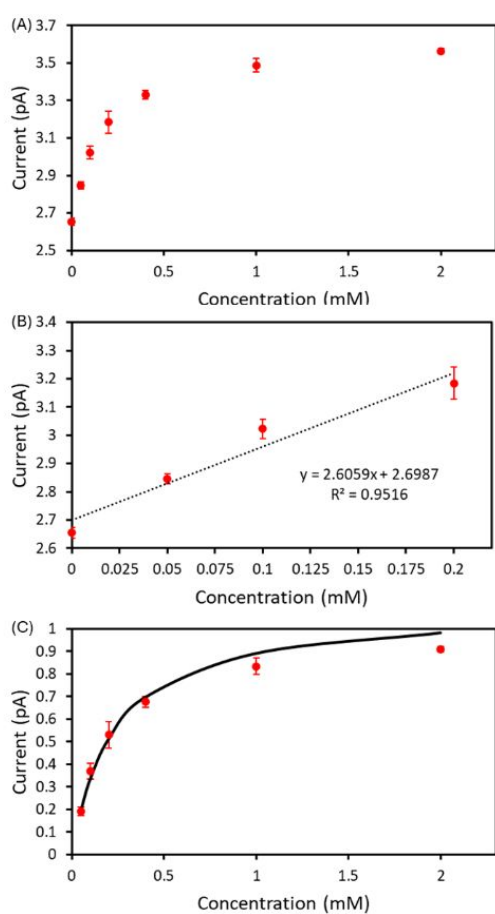


Figure 5. (A) A plot of glutamate detection current on the GluOx-modified Pt nanoelectrode as a function of the glutamate concentration. Y axis is the current measured at $+0.7 \text{ V vs. Ag/AgCl/1M KCl}$ from forward cyclic voltammograms in Figure 4 and x-axis is the concentration of glutamate. (B) Calibration curve at low concentration range (up to $200 \mu\text{M}$), where a linear current-concentration response was observed. (C) The fitting of the background-subtracted experimental current-concentration curve (red square) to Michaelis-Menten curve (black solid line).

A comparison of $2 \text{ mM H}_2\text{O}_2$ and 2 mM glutamate detection on the GluOx-modified Pt nanoelectrode.

To better understand the analytical performance of GluOx-modified Pt nanoelectrodes towards glutamate detection, H_2O_2 with the same concentration as glutamate was added following glutamate detection (Figure 6). Results in Figure 6 showed that GluOx-modified Pt nanoelectrode exhibited a higher current response towards H_2O_2 than Glu of the same concentration. We compared the current at $+0.7 \text{ V vs Ag/AgCl/1 M KCl}$, which is the potential used for calculating glutamate sensitivity and reported to exhibit good H_2O_2 sensitivity. The background-subtracted current corresponding to H_2O_2 produced from 2 mM glutamate is 0.9 pA while for $2 \text{ mM H}_2\text{O}_2$, corresponding current is 9.0 pA .

The sensitivity of the GluOx-modified Pt nanoelectrode towards H_2O_2 detection is 4.5 pA/mM . Biosensor efficiency (BE), which is defined as the ratio of glutamate sensitivity to H_2O_2 sensitivity, is a parameter to measure the efficiency of the enzymatic electrode to convert glutamate to H_2O_2 .²² The glutamate sensitivity is calculated to be 2.6 pA/mM based on the slope of the best linear fit at the linear range of the calibration curve. This leads to a BE of 57.9% . This showed the high efficiency of our Pt nanoelectrode.

Another commonly used parameter to characterize enzymatic electrode is Enz_{act} , which is defined as $I_{\text{max}}/(\text{H}_2\text{O}_2 \text{ sensitivity})$ and used as an indicator of the amount of enzyme loaded on the electrode.²² The Enz_{act} of the GluOx-modified Pt nanoelectrode is 0.243 mM , which is on the same order of magnitude but smaller than the value reported in literature ($2 \text{ mM} - 43 \text{ mM}$).²² This slightly lower Enz_{act} value and K_m value might be related to the small surface area of our nanoelectrode, which leads to a small amount of enzyme loaded on the electrode.

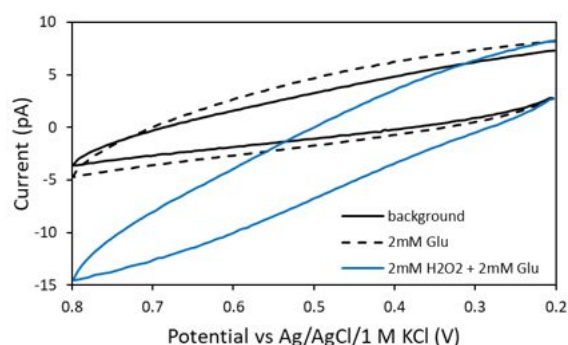


Figure 6. Cyclic voltammograms of the background (black solid curve), 2 mM glutamate with the background (black dashed curve), and $2 \text{ mM H}_2\text{O}_2$ with the 2 mM glutamate and background solution (blue solid curve).

A comparison with GluOx-modified carbon fiber microelectrode.

We further compared the sensitivity of GluOx-modified Pt nanoelectrodes with GluOx-modified carbon fiber microelectrodes (optical and SEM results were shown in Figures 7A and 7B). The results of glutamate detection on a GluOx-modified carbon fiber microelectrode were shown in Figure 7. Figures 7C and 7D showed the CV of the carbon fiber microelectrode in PBS background solution as black dashed curve. After adding different concentrations of glutamate, an increase in current in the potential range of +0.75 V to +1.1 V vs. Ag/AgCl/1 M KCl was observed. Figure 7E showed the calibration curve of glutamate detection on the GluOx-modified carbon fiber microelectrode, which appears to fit well to a Michaelis-Menten like response (solid line). Based on the fitting, this GluOx-modified carbon fiber microelectrode exhibited an I_{\max} of 0.689 nA and a K_m of 301.2 μM towards glutamate detection. The detailed Michaelis-Menten parameter calculation was shown in SI.

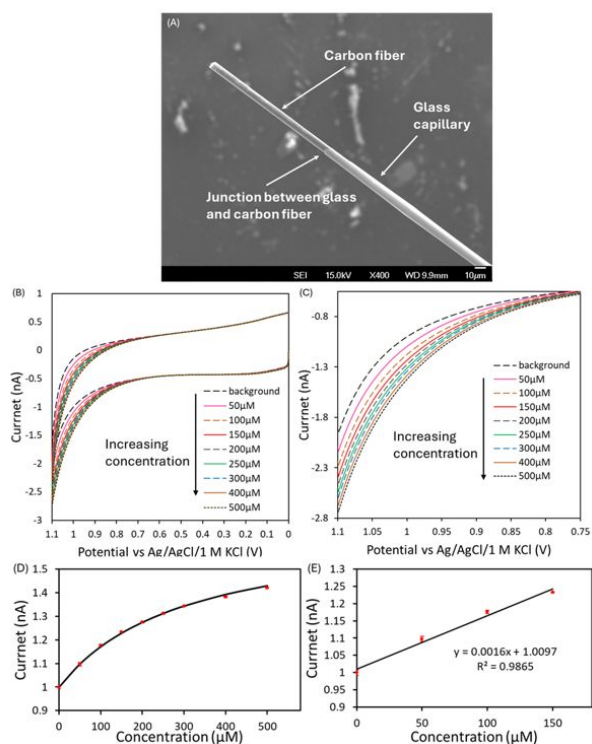


Figure 7. (A) SEM image of a carbon fiber microelectrode (CFE) with a same diameter but different length as the CFE used in Figs B-E, which were prepared in the same batch. (B) Cyclic voltammograms (CVs) of PBS background and glutamate with different concentrations. (C) The forward CVs in the potential range from +0.75 V to +1.1 V vs. Ag/AgCl/1 M KCl, where we can observe a clear increase in current as glutamate concentration increased. (D) Current-concentration plot for glutamate detection (red square), which fits well to the calculated Michaelis-Menten curve (the black curve). (E) Calibration curve at a low concentration range up to 150 μM (red square), which showed a linear response (black solid line).

Current measured at +1.0 V vs Ag/AgCl/1M KCl was used in the calibration curve.

Figure 7F showed the best linear range of the calibration curve is from 50 μM to 150 μM Glutamate. Based on the best linear fit, the calculated sensitivity of the GluOx-deposited carbon fiber microelectrode is 1.6×10^{-3} nA/ μM . The carbon fiber microelectrode has a 7- μm diameter and a sensing length of ~ 350 μm . The optical image of this electrode before enzyme deposition was shown in Figure 7A. A SEM image of a similar carbon fiber microelectrode of a different length was shown in Figure 7B. After taking surface area into account, the area-normalized sensitivity of this GluOx-modified carbon fiber microelectrode is 2.068×10^{-7} nA μM^{-1} μm^{-2} . This sensitivity is lower than the sensitivity of GluOx-modified Pt nanoelectrode (1.057×10^{-5} nA μM^{-1} μm^{-2}).

It is worth noting that in Figures 7C and 7D, the glutamate detection occurred at a higher potential on GluOx-modified carbon fiber microelectrode comparing with GluOx-modified Pt nanoelectrode. The lower sensitivity per area and higher potential requirement for glutamate detection on GluOx-modified carbon fiber microelectrode suggests that Pt is a better material for H_2O_2 sensing than carbon as known in literature. However, we cannot rule out the possible contributing factor from enzyme-deposition methods on the sensitivity variation.

Comparison between different GluOx-modified Pt nanoelectrodes and dip-coating conditions

The GluOx was coated on the electrode via dip-coating with detailed procedures in experimental section. Two electrodes fabricated with slightly different dip-coating conditions showed similar level of sensitivity as shown in Figure S8. They were both dip-coated by dipping in 1% bovine serum albumin (BSA), 0.14% glutaraldehyde (GLDH), followed by dipping in 100 U/mL GluOx, finally followed by dipping in 1% polyethyleneimine (PEI). It was repeated for 15 times for dipping in each solution with a 4-minute air-dry. The SEM images of these two electrodes were shown in Figures 8A and 8C and their corresponding CV curves for HL3 background solution and different concentrations of glutamate were shown in Figures 8B and 8D. Other information such as calibration curve, linear range sensitivity, and Michaelis-Menten parameters calculation were shown in SI. The area-normalized sensitivities are 1.437×10^{-5} nA μM^{-1} μm^{-2} and 3.14×10^{-5} nA μM^{-1} μm^{-2} , respectively.

The current-concentration responses of these two Pt nanoelectrodes were fitted to theory, where Michaelis-Menten parameters were also calculated. The first electrode showed an I_{\max} of 1.067 pA and K_m of 0.354 mM while the second electrode showed an I_{\max} of 2.154 pA and K_m of 0.489 mM. These values are not too far away from that of the first Pt nanoelectrode described above with I_{\max} to be 1.093 pA and K_m to be 0.227 mM.

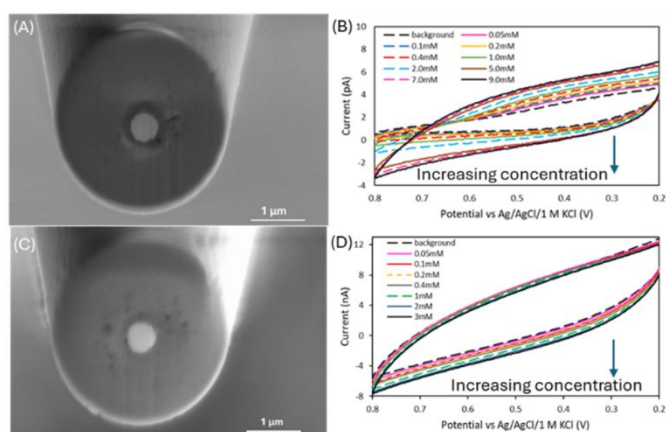


Figure 8. Glutamate detection on a second and third Pt nanoelectrodes. Cyclic voltammograms (CVs) of glutamate detection (B) on a second GluOx-modified Pt nanoelectrode with SEM of the Pt nanoelectrode shown in A; the radius of the Pt nanoelectrode estimated using SEM is 262 nm. CVs of glutamate detection (D) on a third GluOx-modified Pt nanoelectrode with SEM of the Pt nanoelectrode shown in C; the radius of the Pt nanoelectrode estimated using SEM is 264 nm. These two additional Pt nanoelectrodes were fabricated in a similar way as the one in Figure 1B. Concentrations of glutamate were shown in Figure legends.

We would like to point out some of the electrodes did not exhibit glutamate detection after the same enzyme dip-coating process. One possible contributing factor is the presence of the crosslinker used for the immobilization of the enzyme on the electrode surface. These bulky molecules might affect the diffusion of H_2O_2 to the electrode surface. This might also explain why some electrode response did not fit very well to the Michaelis-Menten curve. In addition, the dip-coating involved a drying step in air, which may subject to humidity variations, etc. As a result, it is hard to achieve the exact same dip-coating for different electrodes in air. We may carry out the enzyme-coating in a humidity-controlled chamber in the future. Furthermore, we cannot rule out the possibility of instability occurrence on some electrodes of the deposited-enzyme layer which may be related to the Pt nanoelectrode geometry and coating process. Other possible factors include the variation in the orientation of the enzyme, where Minter *et al.* showed that orientation of the enzyme on the electrode surface affects the sensing performance.¹²

Experimental

Reagents

Sodium chloride (NaCl) was from EMD Chemicals (Gibbstown, NJ). Potassium chloride (KCl) was from VWR International (Radnor, PA). Calcium chloride dihydrate ($\text{CaCl}_2 \cdot 2\text{H}_2\text{O}$), bovine serum albumin (BSA), glutaraldehyde (GLDH), L-glutamate, sodium bicarbonate (NaHCO_3), and sucrose were obtained from Sigma-Aldrich (St. Louis, MO). Magnesium chloride hexahydrate ($\text{MgCl}_2 \cdot 6\text{H}_2\text{O}$) was from Amresco (Solon, OH). Agar, 4-(2-hydroxyethyl)-1-piperazineethanesulfonic acid (HEPES), sodium perchlorate

(NaClO_4), and trehalose were from Fisher Scientific (Pittsburg, PA). Hexaamineruthenium (III) chloride (RuHex) was from Strem Chemicals Inc. (Newburyport, MA). Glutamate oxidase was from Cosmo Bio USA (Carlsbad, CA). All aqueous solutions were prepared from 18.3 M Ω cm deionized water. Phosphate buffered saline (PBS) was prepared by dissolving 1 PBS tablet in 200 mL deionized water. The PBS solution contains 137 mM NaCl, 2.7 mM KCl, 10 mM Na_2HPO_4 1.8 mM KH_2PO_4 . The haemolymph-like solution (HL3) used was an aqueous solution containing 70 mM NaCl, 5 mM KCl, 1.5 mM $\text{CaCl}_2 \cdot \text{H}_2\text{O}$, 20 mM $\text{MgCl}_2 \cdot 6\text{H}_2\text{O}$, 10 mM NaHCO_3 , 5 mM trehalose, 115 mM sucrose, and 5 mM HEPES.²³

Fabrication and functionalization of Pt nanoelectrodes

Pt nanoelectrodes were fabricated by pulling Borosilicate capillaries (Sutter Instruments Co. Novato CA; 1 mm outer diameter, 0.2 mm inner diameter, 10 cm length) containing Pt wires (Goodfellow Corp. Pittsburgh PA; 0.025mm) using a P-2000 laser puller (Sutter Instruments, Novato, CA). Borosilicate capillaries were soaked in piranha solution overnight to remove any organic moieties. The capillaries were then flushed with DI water and acetone before being dried in a vacuum oven for a minimum of 2 hrs under active vacuum at a temperature of at least 150°C. Approximately 2 cm long Pt wires were threaded into and centered within the capillaries before being pulled in the P-2000 laser puller. Each capillary was subjected to an active vacuum during pulling by attaching tubing to each end of the capillary connected to a vacuum pump.

Each Pt nanoelectrode was pulled in three stages.²⁴ In the first step, the capillary was thinned using a single program [Heat: 390, Filament: 4, Velocity: 15, Delay: 120, Pull: 0] that looped 4 times before aborting the program. Following the first step, two stoppers were added to the puller to prevent the puller bars from separating and a second program [Heat: 280, Filament: 4, Velocity: 12, Delay: 120, Pull: 0] was run for exactly 10 seconds before aborting it. This second program sealed the platinum within the glass. Finally, the stoppers were carefully removed, and the capillary was separated into 2 electrodes by a third program [Heat: 230, Filament: 3, Velocity: 22, Delay: 120, Pull: 15].

The electrodes were optically characterized to confirm that there were no visible gaps between the platinum wire and glass, and to roughly estimate the electrode size. Electrodes were finished by coating the tip of a sanded 0.15mm Cu wire with silver conductive epoxy (Ted Pella Redding Ca) and establishing contact between the Cu wire and the Pt wire. This connection was made while using precautions (e.g., grounded and wearing equipment) to protect against electrostatic discharge (ESD) to avoid damaging the tip of the Pt nanoelectrode using procedures reported.^{25, 26} The same ESD protection was used when handling all the Pt nanoelectrodes. The epoxy was cured for at least 30 min at 100°C. The electrodes were electrochemical characterized, then milled using a SEM/FIB instrument (FEI Helios 600i Dual Beam SEM/FIB, FEI Co., Hills-boro, OR) using a 3 kV accelerating voltage and a beam current of 5.4 pA to produce a platinum disk-like nanoelectrode. For the SEM images in Figure 1B, the shape appeared to be oval, and the average size of the long and short axes were used to estimate the size of the

electrode. The SEM images were taken at a tilt of 52°, and the tilt-corrected images were presented here.

After the milled electrode was recharacterized, it was coated with an enzyme film for functionalization. A functionalization solution of 0.9% (wt%) BSA, 0.126% (wt%) glutaraldehyde, and 100 U/mL glutamate oxidase was prepared, and each electrode was carefully dipped into the solution anywhere between 15 and 30 times, allowing the electrode to sit in the solution for 15s before removing to dry a layer for another 15s. The film was allowed to cure at room temperature for an additional 72 hours before glutamate sensing to ensure sufficient binding to the electrode surface.

An alternative method for functionalization was dip-coating in three solutions. 1% BSA + 0.14% glutaraldehyde (GLDH) solution, 100 U/mL GluOx solution, and 1% PEI solution were prepared separately. The electrode was firstly dipped into the BSA/GLDH solution, then dipped into the GluOx solution, finally dipped into the PEI solution. Each time of dip lasted several seconds, then the electrode was taken out to dry in air for ~4 min. The dip repeated for 15 times for each concentration. The electrode was also kept under room temperature for ~72 hours for the film to cure before use.

Fabrication and functionalization of carbon fiber microelectrodes

7- μm diameter carbon fiber (Goodfellow Corp., Pittsburgh, PA) was aspirated into a glass capillary, then the glass capillary was pulled with a laser-puller. The pulled microelectrodes were inspected under microscope. Electrodes with a good seal at the junction between the glass tip and carbon fiber were further processed. A scalpel was used to trim the exposed carbon fiber to the desired length (100-300 μm) to generate the carbon fiber microelectrode. Finally, a conductive wire (OK industries, Tuckahoe, NY) coated with silver paint (GC electronics, Miami, FL) was inserted into the glass capillary and connected with the carbon fiber at the back.

The carbon fiber electrode was then deposited with GluOx by dip-coating in an enzyme solution composed of 0.04 U/ μL GluOx, 0.0096 g/mL BSA, and 0.0096 g/mL PEI. Prior to the dip-coating step, the carbon fiber electrode was electrochemically conditioned with fast scan cyclic voltammetry for 10 minutes with a triangular waveform ranging from -0.4 V to +1.3 V vs. an Ag/Ag wire with a scan rate of 400 V/s and a frequency of 10 Hz. The conditioned carbon fiber microelectrode was dipped in the GluOx/BSA/PEI solution for 15 times. Each time of dipping, the electrode was immersed in the solution for 2 mins then taken out in air for 30 seconds to dry. Finally, the electrode was stored under room temperature for ~24 hours before use to allow the film to cure.

Electrochemical characterization

All electrochemical measurements were performed using either a CHI 760E or CHI 920D potentiostat (CH Instruments, Austin, TX). Cyclic voltammetry (CV) was used to study the detection of glutamate. A three-electrode configuration was used. The working electrode was the Pt nanoelectrode or the carbon fiber microelectrode. The reference electrode was a commercial Ag/AgCl

electrode filled with 1M KCl solution placed in a solution of HL3 (or PBS) separated by a salt bridge. The counter electrode was a W wire electrode. During Pt characterization, applied negative potentials yielded reduction of the ruthenium hexamine (III) $[\text{Ru}(\text{NH}_3)_6]^{3+}$ to ruthenium hexamine (II) $[\text{Ru}(\text{NH}_3)_6]^{2+}$ presented as a positive current (Cell 1). The measured current was used to determine the electrochemical size of the nanoelectrode. Glutamate detection experiments on the Pt nanoelectrode and the carbon fiber microelectrode were carried out using the configuration presented in Cell 2 and Cell 3, respectively.

Cell 1. Pt | HL3 + x mM RuHex || HL3 | 1 M KCl | AgCl | Ag

Cell 2. Pt | HL3 + x mM L-Glutamate || HL3 | 1 M KCl | AgCl | Ag

Cell 3. C | PBS + x mM L-Glutamate || PBS | 1 M KCl | AgCl | Ag

Data analysis

The Michaelis-Menton equation shown below describes the relationship between the analyte concentration (c) and the reaction rate (v).

$$v = \frac{v_{max} c}{K_m + c} \quad (3)$$

v_{max} is the maximum reaction rate, K_m is the Michaelis constant which is defined as the analyte concentration that gives half of the v_{max} . They are both constant parameters related to the property of the enzyme and the electrode.

The reaction rate v (same as flux with a unit of $\text{mol cm}^{-2} \text{s}^{-1}$) is related to current (i) as the following equation.

$$v = \frac{i}{nFA} \quad (4)$$

n is the number of electrons, F is Faraday constant, A is surface area of the electrode, they are all constants. Considering nFA is a constant, Equation (1) can be rewritten as:

$$i = \frac{i_{max} c}{K_m + c} \quad (5)$$

In order to solve for i_{max} and K_m , the reciprocal of equation (3) is considered as shown below.

$$\frac{1}{i} = \frac{K_m + c}{i_{max} c} = \frac{K_m}{i_{max} c} + \frac{1}{i_{max}} \quad (6)$$

By plotting $1/i$ as a function of $1/c$, the slope of this curve is K_m/i_{max} , and the intercept of this curve is $1/i_{max}$. Thus, from the slope and intercept, both K_m and i_{max} can be determined. Using the results in Figure S1 as an example, the i_{max} is calculated to be 1.093 pA, the K_m is calculated to be 0.227mM.

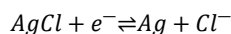
Biosensor sensitivity (BE)²² is a measurement of efficiency of the electrode to convert analyte to H_2O_2 . It is defined as the ratio between analyte sensitivity and H_2O_2 sensitivity. The sensitivity of analyte, glutamate in our case, is defined as the slope linear concentration range of the calibration curve.

$$BE = \frac{\text{Glu sensitivity}}{\text{H}_2\text{O}_2 \text{ sensitivity}} = \frac{\text{Glu linear range slope}}{\text{H}_2\text{O}_2 \text{ sensitivity}} = \frac{2.6059 \text{ pA/mM}}{4.5 \text{ pA/mM}} = 57.9\%$$

The enzyme activity Enz_{act} is an indication of active enzyme loading on the electrode.²² It is defined as the maximum current (i_{max}) calculated from equation (4) normalized to H_2O_2 sensitivity.

$$Enz_{act} = \frac{i_{max}}{H_2O_2 \text{ sensitivity}} = \frac{1.093 \text{ pA}}{4.5 \text{ pA/mM}} = 0.243 \text{ mM}$$

The reference electrode potential was calculated from the Nernst equation.²⁷ Considering the following reaction:



The reference electrode potential is related to Cl^- concentration:

$$E_{Ag/AgCl} = E_{Ag/AgCl}^{\theta'} - \frac{RT}{nF} \ln[Cl^-] \quad (7)$$

R is ideal gas constant, n is the number of electrons, which is 1 in this case, F is Faraday constant.

Considering room temperature $T = 25 \text{ }^\circ\text{C}$, we can plug in all these constants, the equation can be rewritten as:

$$E_{Ag/AgCl} = E_{Ag/AgCl}^{\theta'} - 0.05916 \log[Cl^-] \quad (8)$$

For 1 M KCl solution, $[Cl^-] = 1$,

$$E_{Ag/AgCl}^{1M \text{ KCl}} = E_{Ag/AgCl}^{\theta'} - \frac{RT}{nF} \ln[Cl^-] = E_{Ag/AgCl}^{\theta'} \quad (9)$$

For 0.1 M PBS solution, $[Cl^-] = 0.014 \text{ M}$,

$$E_{Ag/AgCl}^{0.1M \text{ PBS}} = E_{Ag/AgCl}^{\theta'} - \frac{RT}{nF} \ln[Cl^-] = E_{Ag/AgCl}^{\theta'} + 0.11 \text{ V} \quad (10)$$

For 0.6 V vs Ag/AgCl in 0.1 M PBS,

$$E = 0.6 \text{ V} + E_{Ag/AgCl}^{0.1M \text{ PBS}} = 0.71 \text{ V} + E_{Ag/AgCl}^{\theta'} = 0.71 \text{ V} + E_{Ag/AgCl}^{1M \text{ KCl}}$$

Therefore, +0.6 V vs Ag/AgCl in 0.1 M PBS is the same as +0.71 V vs Ag/AgCl/1 M KCl.

Two-sample t-test was conducted with MatLab to check if there is significant change in current after adding glutamate. Briefly speaking, we performed three repeated CVs for each concentration during data collection. Then the current at +0.7 V vs Ag/AgCl/1M KCl of these repeated CV runs was used for the t-test. The hypothesis to test is if the current at +0.7 V of adjacent glutamate concentrations comes from the same group. For example, the repeated background (0 mM glutamate) CVs showed the current of 2.655, 2.677, and 2.631 pA, and the repeated CVs at 0.05 mM of glutamate showed the current of 2.826, 2.842, and 2.870 pA. Then the two-sample t-test was performed to determine if these two groups of number come from the same group. As a result, a p-value less than 0.001 was calculated from MatLab, indicating that these two groups of number are significantly different. Similarly, the current at +0.7 V for the three repeated CVs at other concentrations of glutamate were also used for the t-test. The box plot and corresponding p-values between adjacent glutamate concentrations were shown in Figure S4.

Conclusions

We have studied glutamate detection on the GluOx-modified Pt nanoelectrode with a planar geometry for the first time. Detection of glutamate was observed at a similar potential as reported in the literature for glutamate detection. The current-concentration curve fitted well to a Michaelis-Menten curve,

and a linear response was observed at a low concentration range of glutamate. A similar K_m and I_{max} were observed for three different GluOx-modified Pt nanoelectrodes. Future work will be needed to further develop the GluOx-modified Pt nanoelectrodes, for instance, by controlling the orientation of the enzymes on the electrode surface to allow a better sensing performance.

Author contributions

Supervision: M.S.; Conceptualization and methodology: H.J., P.X., R.C. and M.S.; Data collection: H.J. and P.X.; Data analysis: P.X., H.J. and M.S.; Manuscript writing: P.X., H.J., and M.S.; Project administration: M.S.; Funding acquisition: M.S. All authors reviewed the manuscript.

Conflicts of interest

There are no conflicts to declare.

Data availability

The data presented in this study are available on request from the corresponding author. The data supporting this article have been included as part of the Supplementary Information.

Acknowledgements

We are grateful for the support of this research by U.S. National Science Foundation grant (CMMI 1935181) and Scialog grant (#SA-MND-2023-033a) from Research Corporation for Science Advancement and the Paul G. Allen Frontiers Group. The SEM and FIB experiments were carried out in the Materials Research Laboratory Central Research Facilities, University of Illinois at Urbana-Champaign. Financial support for this publication results from Scialog grant #SA-MND-2023-033a from Research Corporation for Science Advancement and the Paul G. Allen Frontiers Group

References

1. R. Anwyl and P. Usherwood, *Nature*, 1974, **252**, 591-593.
2. P. Usherwood and P. Machili, *Journal of Experimental Biology*, 1968, **49**, 341-361.
3. H. Gerschenfeld, *Physiological Reviews*, 1973, **53**, 1-119.
4. D. R. Curtis and G. A. Johnston, *Ergebnisse der Physiologie Reviews of Physiology, Volume 69*, 1974, 97-188.
5. K. Krnjević, *Nature*, 1970, **228**, 119-124.
6. T. V. Bliss and T. Lømo, *The Journal of physiology*, 1973, **232**, 331-356.
7. V. F. Castellucci, E. R. Kandel, J. H. Schwartz, F. D. Wilson, A. C. Nairn and P. Greengard, *Proceedings of the National Academy of Sciences*, 1980, **77**, 7492-7496.
8. R. G. Morris, E. Anderson, G. S. Lynch and M. Baudry, *Nature*, 1986, **319**, 774-776.

9. J. W. Murrough, C. G. Abdallah and S. J. Mathew, *Nature Reviews Drug Discovery*, 2017, **16**, 472-486.
10. J. Schultz, Z. Uddin, G. Singh and M. M. Howlader, *Analyst*, 2020, **145**, 321-347.
11. E. R. da Silva Moraes, A. B. A. Grisolia, K. R. M. Oliveira, D. L. W. Picanço-Diniz, M. E. Crespo-López, C. Maximino, E. d. J. O. Batista and A. M. Herculano, *Journal of Chromatography B*, 2012, **907**, 1-6.
12. R. D. Milton, T. Wang, K. L. Knoche and S. D. Minter, *Langmuir*, 2016, **32**, 2291-2301.
13. C. Pan, H. Wei, Z. Han, F. Wu and L. Mao, *Current Opinion in Electrochemistry*, 2020, **19**, 162-167.
14. Y. Hu, K. M. Mitchell, F. N. Albahadily, E. K. Michaelis and G. S. Wilson, *Brain research*, 1994, **659**, 117-125.
15. M. Marquitan, M. D. Mark, A. Ernst, A. Muhs, S. Herlitze, A. Ruff and W. Schuhmann, *Journal of materials chemistry B*, 2020, **8**, 3631-3639.
16. C. Lefrou, *Journal of Electroanalytical Chemistry*, 2006, **592**, 103-112.
17. J. E. Baur and R. M. Wightman, *Journal of electroanalytical chemistry and interfacial electrochemistry*, 1991, **305**, 73-81.
18. E. Naylor, D. V. Aillon, S. Gabbert, H. Harmon, D. A. Johnson, G. S. Wilson and P. A. Petillo, *Journal of Electroanalytical Chemistry*, 2011, **656**, 106-113.
19. X. K. Yang, F. L. Zhang, W. T. Wu, Y. Tang, J. Yan, Y. L. Liu, C. Amatore and W. H. Huang, *Angewandte Chemie*, 2021, **133**, 15937-15942.
20. L. C. Kimble, J. S. Twiddy, J. M. Berger, A. G. Forderhase, G. S. McCarty, J. Meitzen and L. A. Sombers, *ACS sensors*, 2023, **8**, 4091-4100.
21. S. Govindarajan, C. J. McNeil, J. P. Lowry, C. P. McMahon and R. D. O'Neill, *Sensors and Actuators B: Chemical*, 2013, **178**, 606-614.
22. R. Ford, S. J. Quinn and R. D. O'Neill, *Sensors*, 2016, **16**, 1565.
23. B. Stewart, H. Atwood, J. Renger, J. Wang and C.-F. Wu, *Journal of Comparative Physiology A*, 1994, **175**, 179-191.
24. M. A. Mezour, M. Morin and J. Mauzeroll, *Analytical chemistry*, 2011, **83**, 2378-2382.
25. R. Chen, K. Hu, Y. Yu, M. V. Mirkin and S. Amemiya, *Journal of The Electrochemical Society*, 2015, **163**, H3032.
26. N. Nioradze, R. Chen, J. Kim, M. Shen, P. Santhosh and S. Amemiya, *Analytical chemistry*, 2013, **85**, 6198-6202.
27. A. J. Bard, L. R. Faulkner and H. S. White, *Electrochemical methods: fundamentals and applications*, John Wiley & Sons, 2022.

Enzyme-modified Pt nanoelectrodes for glutamate detection

Peibo Xu^{†,a}, Henry David Jetmore^{†,a}, Ran Chen^{a, b}, Mei Shen^{a,*}

a. Address: Department of Chemistry, University of Illinois at Urbana Champaign, Urbana, IL, 61801, USA

b. Current address: School of Chemistry and Chemical Engineering, Southeast University, Nanjing, 211189, China.

†. Equal contribution, co-first author

*. Corresponding author, E-mail address: mshen233@illinois.edu

The data supporting this article have been included as part of the Supplementary Information.